Appendix B

Crack Driving Force and Growth Rate Estimates

Appendix B – Crack Driving Force and Growth Rate Estimates

Fracture mechanics analysis techniques were applied to estimate crack-tip stress intensity factors (K) and crack growth times for postulated flaws in the Nozzle-3 J-groove weld and adjacent nozzle wall. Calculations were performed using the NASCRAC™ Software[1], a commercially available, general-purpose fracture mechanics analysis program developed by Exponent for NASA. Weight-function (or influence function) K-solutions in the NASCRAC program calculate K-values as a function of crack size, crack shape, and the stress distribution at the crack location in the un-cracked body. Because the weight-function crack solutions use stress from the un-cracked bode, stresses for K-calculation can be readily obtained from finite element analysis without having to explicitly model cracks. For the Nozzle-3 cracking analysis, the complete bivariate hoop stress distribution through the nozzle wall and weld was obtained from the finite element analysis described in Appendix A.

Two separate influence-function crack models were employed, a four-degree-of-freedom (4-DOF) buried elliptical crack, shown schematically in Figure 1, and a three-degree-of-freedom (3-DOF) semi-elliptical surface crack, shown schematically in Figure 2. Each semi-minor and semi-major axis tip of the buried ellipse or surface semi-ellipse is a degree-of-freedom (DOF) in the influence function models. A separate K and growth rate is calculated for each DOF, or crack tip, so during a simulation a growing crack can change shape based on the relative growth rates at the different crack tips.

Although the final geometry of Crack 1 in CRDM Nozzle 3 and J-groove weld does not lend itself well to idealization with either the buried elliptical crack solution or the surface semi-ellipse, these two crack models can be used to accurately evaluate the growth of smaller cracks representing earlier stages of PWSCC growth in the weld and nozzle wall. Using a high-refinement area integration option in the NASCRAC program, these elliptical crack models can also be used to obtain reasonable and conservative estimates of K for larger crack sizes, even where small regions of the postulated elliptical or semi-elliptical crack pass outside the cracked body, as will be discussed further below. In such cases, zero values of stress are input to the

program in the areas outside the body, so that there is no contribution to the integrated K results from those areas. This approximation technique typically results in under-prediction of K values because no account is taken of the elevating effect on K of the extra free surfaces intersecting the crack. For example, the K values from the buried elliptical crack model used for growth from the bottom of the weld will be lower (by about 10-12%) than the actual re-entrant corner crack being simulated because the actual crack has two free surfaces, which will elevate K relative to a completely buried crack under the same loading.

All growth life estimates in the cases presented herein are based on the Davis-Besse Alloy-600 PWSCC crack growth rate[2] (CGR) fit. As shown in Figure 3, the EPRI/MRP disposition curve for Alloy-182 weld metal[3] falls nearly on top of the Davis-Besse Alloy-600 curve, and in fact, slightly above it, especially at lower crack driving forces. For conservatism in this analysis, the Davis-Besse Alloy-600 CGR relation was used for both nozzle and weld-metal growth simulations. Although the tested Alloy-182 material from Davis-Besse Nozzle 11 exhibited lower than expected growth rates, the cracking experience at Davis-Besse and Oconee demonstrates the high variability in PWSCC cracking. The extent of cracking observed in Nozzles 2 and 3, and particularly in the J-groove weld of Nozzle 3, clearly suggests a greater susceptibility to PWSCC growth than in Nozzle 11. Therefore, the Alloy-600 CGR relation was deemed appropriate for use in simulation of Nozzle-3 weld and nozzle cracking growth.

One of the most highly stressed locations in the J-groove weld, based on the finite element analysis results, was at the bottom of the weld close to the OD of the nozzle wall. This location is directly exposed to primary coolant water, and thus would have been a likely spot for PWSCC crack initiation at Nozzle 3. Figure 4 shows the results of a crack-growth simulation that postulated an initial crack, 0.01-inch in radius, located at the bottom of the weld at the nozzle OD. As indicated above, the K-values in this simulation will be low due to the fact that the buried-elliptical crack model does not include free-surface effects on K. Thus, the predicted crack growth rates are expected to be lower than actual, and the time to grow the crack through-wall was shorter than predicted.

The general shape of the simulated crack shown in Figure 4 is consistent with the general shape of cracks in Davis-Besse Nozzles 2 and 3 in that the actual nozzle cracks suggest more rapid

growth in the highly stressed J-groove weld with subsequent growth from the weld into the nozzle wall from the OD. The UT profile of Crack 1 in Nozzle 2^4, as shown in Figure 5, is a good example of this growth pattern and likely resembles the middle stage of growth of Crack 1 in Nozzle 3.

Another crack shape that suggests weld cracking as well as nozzle cracking can be seen in the profile of Crack 4 in Nozzle 3, shown in Figure 6. Crack 4 in Nozzle 3 appears to have grown from the weld toward the ID of the nozzle; however, in this case, another crack appears to have initiated on the ID surface of the nozzle and grown outward toward the larger crack. Two more similar examples of OD and ID initiated cracks growing toward one another can be seen in the UT profiles of Cracks 4 and 10 of Nozzle 2 (see Reference 4) The presence of the larger cracks likely raised the stress at the ID of the nozzle wall above the weld sufficiently to initiate ID cracks. Based on the crack driving force and growth rate calculated for the postulated crack in Figure 4, the two cracks shown in Figure 6 would likely have grown together (i.e., linked up) in a matter of months, had they not been removed from service in February 2002. The UT examinations could not reliably detect, or "see," cracking in the J-groove welds beyond the OD of the nozzle walls; yet, cracking profiles like those shown in Figure 5 and Figure 6 strongly suggest that the J-groove welds were also cracked, especially in light of the fact that much of the industry data for PWSCC growth in Alloy 182 shows higher CGRs, on average, than in Alloy 600.

Figure 7 shows results from a simulation that postulated a long, shallow, axial crack at the highest stress location on the ID surface of the nozzle, which is slightly above the top of the weld. The ID hoop stress in that region from the finite element analysis is 36 ksi under operating conditions. This type of long, shallow crack can develop as a result of link-up of a number of smaller, collinear, ID PWSCC crack initiations. Growth from the initial 0.03-inch depth to break-through at the top of the weld is predicted to take just over three years, ignoring any link-up with other cracks. However, the profile of Nozzle-3 Crack 4, shown in Figure 6, clearly indicates how multiple cracks could link up and increase overall crack size in a short period of time, much less than predicted by assuming growth of only a single crack. This is further supported by the analysis results. The ID-crack growth schematic in Figure 7 includes

an overlaid outline of the weld-bottom crack from Figure 4. This comparison indicates that two such cracks, one growing from the highest stress location on the OD and one growing from the highest stress location on the ID, could readily link up to form a single, much larger crack in roughly three years time. The magnitude of K at the upper and lower crack tips of the combined crack would be greater than that of the two individual cracks prior to link up, and thus, the crack growth rates would increase after link up.

As mentioned previously, the final observed profile of Crack 1 in Nozzle 3 does not lend itself well to idealization with either a buried elliptical crack model or a surface semi-elliptical crack model. However, these models can be used to conservatively estimate the crack driving force, and thus the CGR, at the upper tip of Crack 1 in Nozzle 3 as it grew above the top of the J-groove weld. Figure 8 shows calculated K-values for a series of semi-elliptical cracks of increasing length above the top of the weld. The lower crack tip of each crack was held fixed at 1.2 inches below the bottom of the weld and the crack depth measured from the nozzle ID was held constant at one inch, well into the weld. As was done with the buried elliptical crack simulation of weld-bottom crack growth, the regions of this large crack that extend outside the nozzle wall and weld were assigned zero values of stress for the weight-function integration of K. For comparison, the actual final size of Crack 1 in Nozzle 3 was larger than the largest of these postulated cracks. It extended 1.2 inches above the weld and 1.6 inches below the weld, almost to the end of the nozzle, and deeper into the weld. Several different crack lengths were chosen for analysis to examine the variation in crack driving force with crack length above the top of the weld. The predicted crack driving force, K, at the upper crack tip under operating conditions ranged from 53 ksi $in^{1/2}$ when the upper tip was even with the top of the weld down to 24 ksi $in^{1/2}$ for a crack extending to 1.2 inches above the top of the weld. These K values were used to interpolate corresponding crack growth rates for the Davis-Besse Nozzle-3 Alloy 600 using the curve shown in Figure 3.

Figure 9 shows PWSCC growth rates for the upper tip of a long axial crack in the nozzle wall based on interpolation in Figure 3 using the calculated crack driving force values shown in Figure 8. Also plotted are the K-values themselves as a function of crack length above the weld. We expect the actual K-values and corresponding CGR at the upper tip were greater than

predicted for the latter stages of growth, due to the larger size of Nozzle-3 Crack 1 compared to this approximation. This would be the case until late in the development of the head wastage cavity when loss of head material behind the weld likely reduced the residual stress level in the J-groove weld, as was predicted by a DEI simulation[5]. These estimates of growth rate for the upper end of the long axial crack in Nozzle 3 are substantially greater than any prior estimates by others, yet they are consistent with the measured growth rates for Nozzle-3 material, the large size of the observed crack, and the high weld and nozzle stresses predicted by our analysis, as well as similar analyses by others[6,7,8].

The interpolated crack growth rates shown in Figure 9 were integrated to obtain estimates of the time to grow the upper crack tip in Nozzle 3 to various heights above the top of the weld, thus creating a leakage path. Figure 10 plots growth time in effective full-power years (EFPY) as a function of crack length above the top of the weld. These results indicate that all of the growth above the top of the weld of Crack 1 in Nozzle 3 at Davis-Besse likely occurred in less than three EFPY.

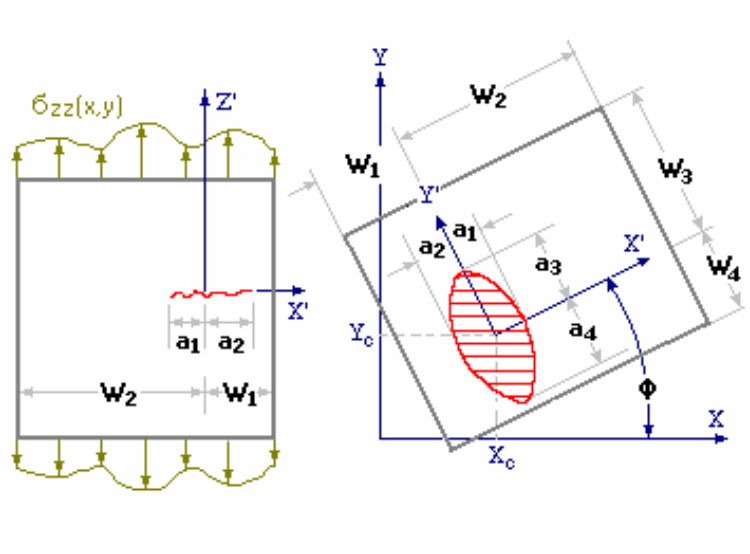

Figure 1. Schematic of four-degree-of-freedom model for a buried elliptical crack from the NASCRAC Software.

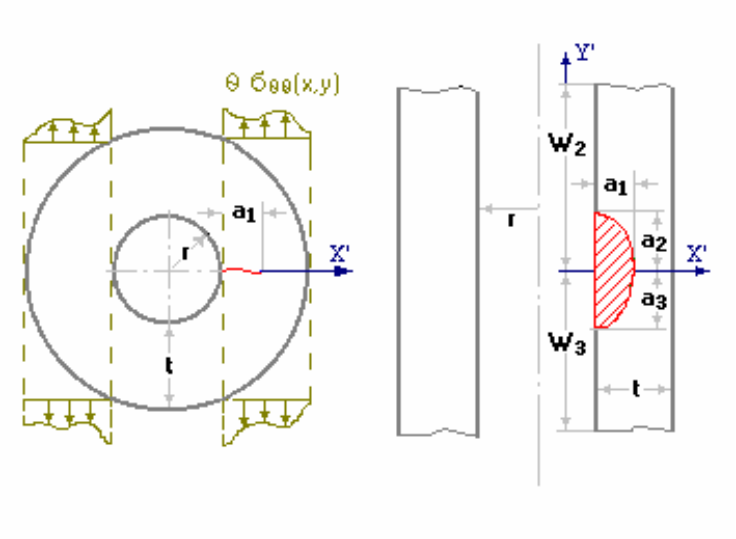

Figure 2. Schematic of three-degree-of-freedom model of a semi-elliptical surface crack in a cylinder from the NASCRAC Software.

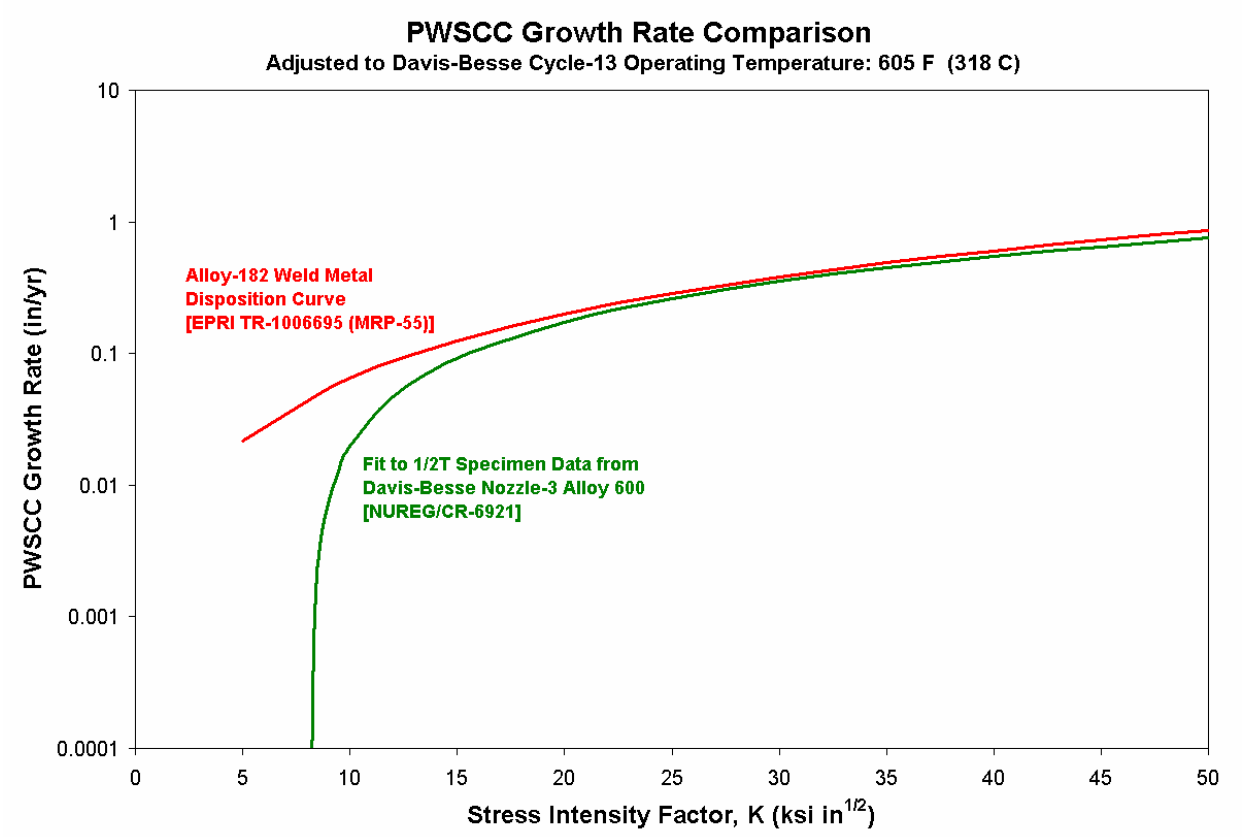

Figure 3. Comparison of PWSCC crack growth rate curve fit for Alloy 600 from Davis-Besse Nozzle 3 to EPRI/MRP Alloy-182 disposition curve.

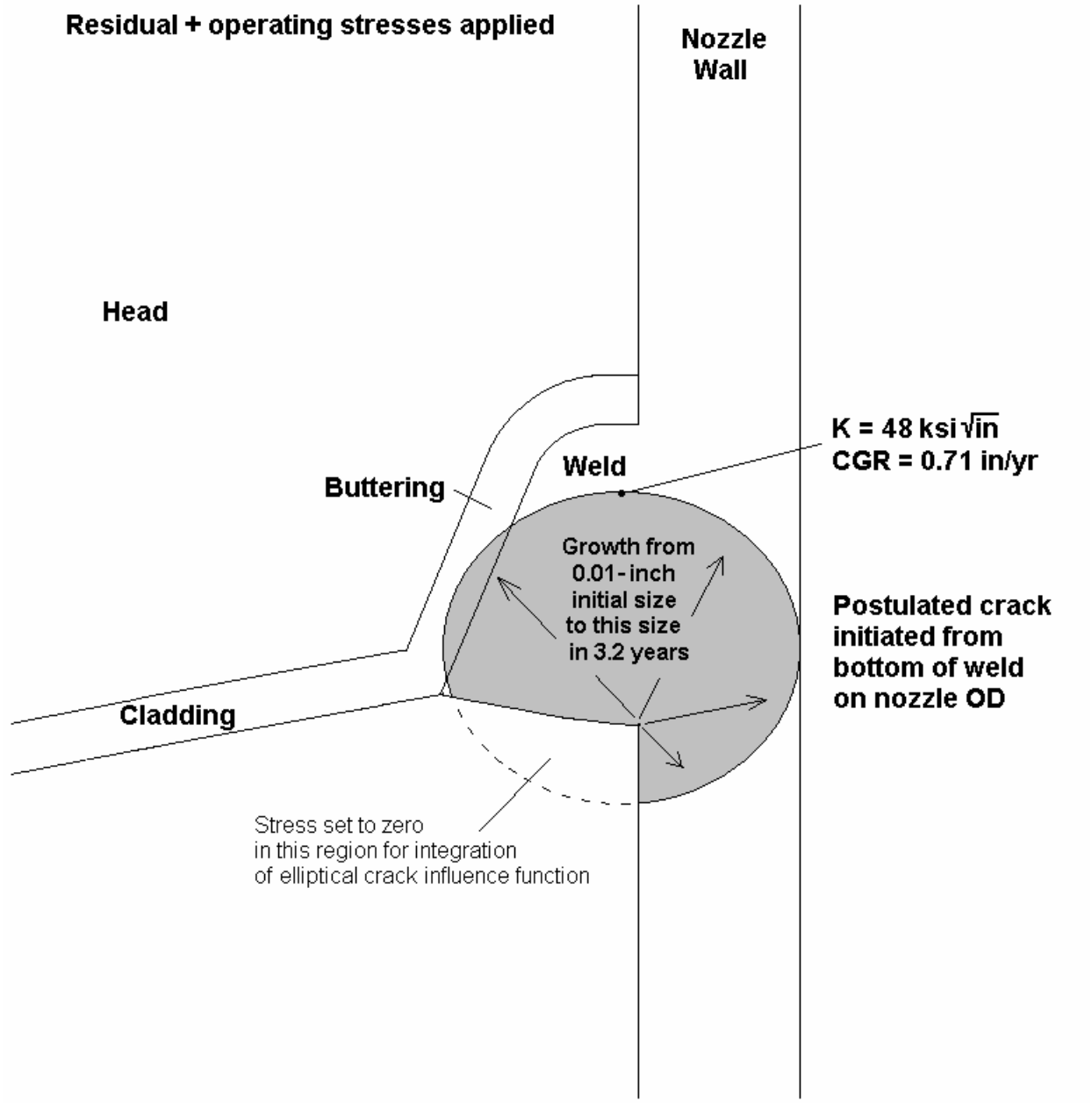

Figure 4. Simulation of PWSCC growth from a postulated 0.010-inch initial crack at the bottom of the weld on the nozzle OD. Break-through to nozzle ID predicted in 3.2 years.

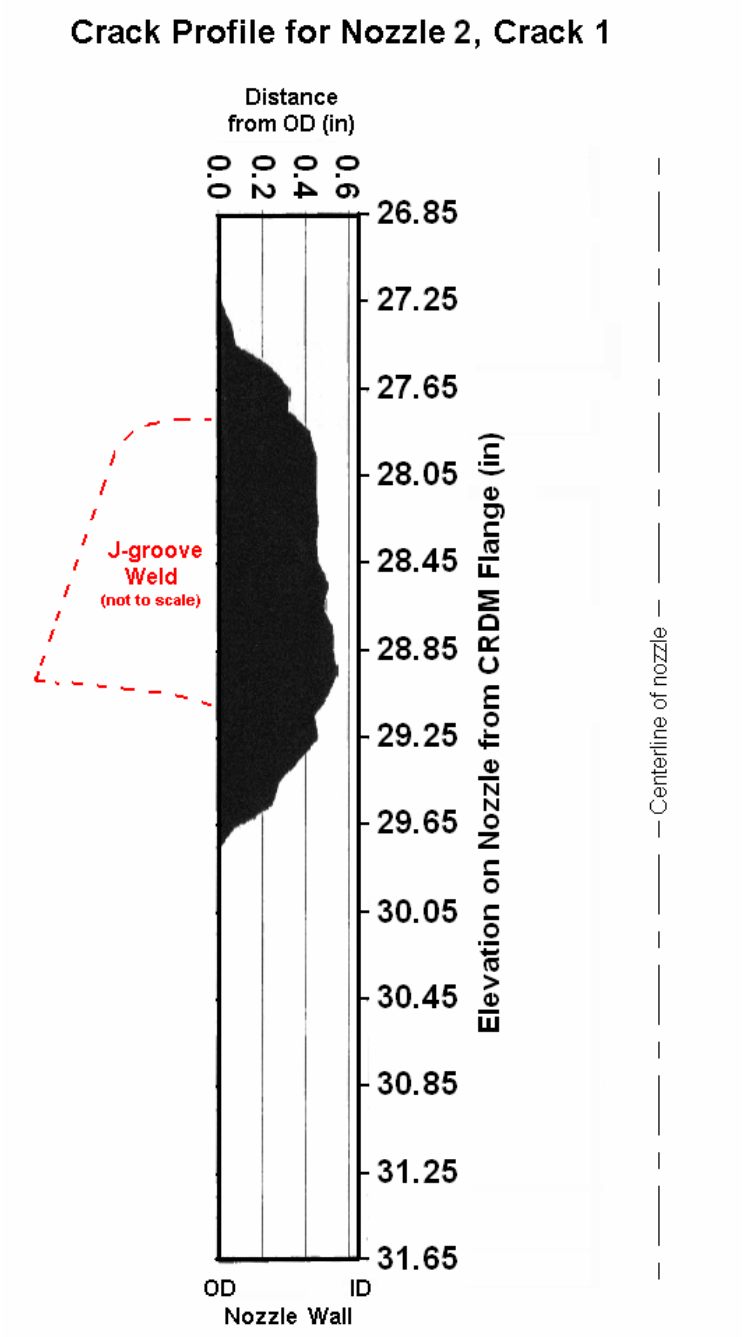

Figure 5. Proportionally scaled UT profile of Crack 1 in Nozzle 2 based on Framatome UT examination results. [Adapted from Reference 4.]

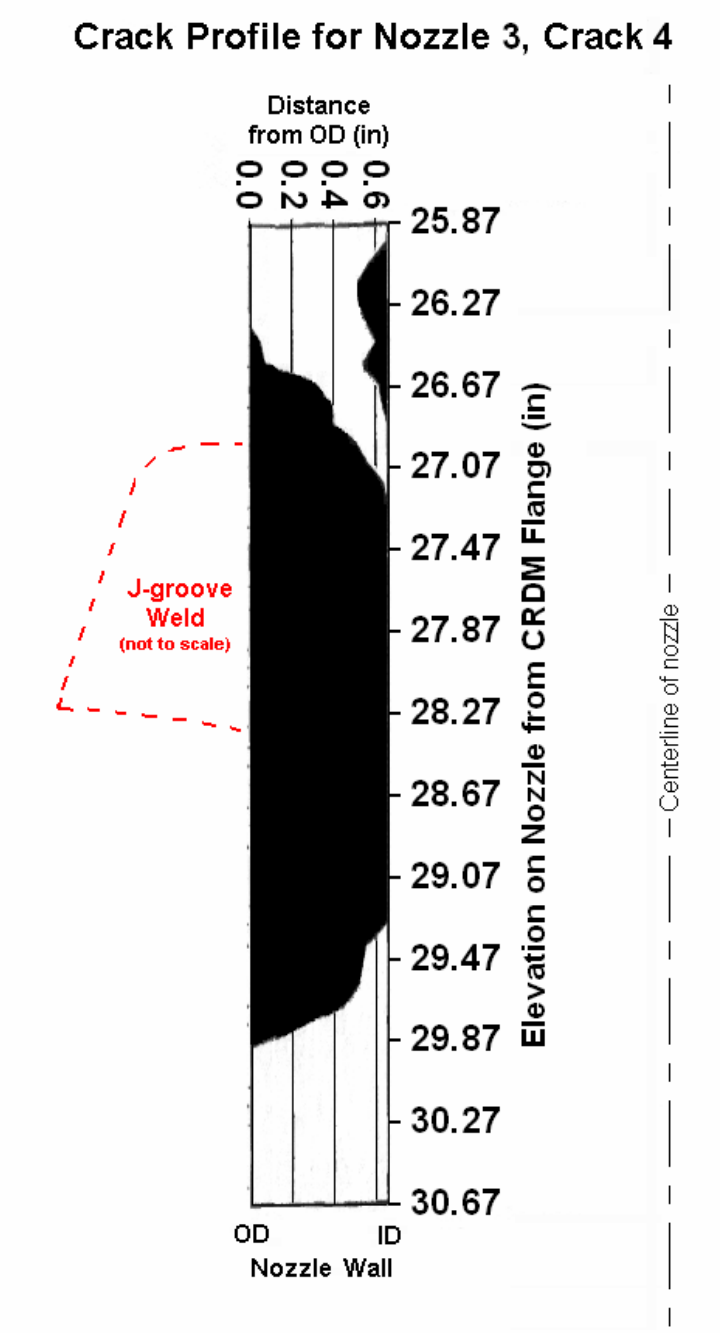

Figure 6. Proportionally scaled UT profile of Crack 4 in Nozzle 3 based on Framatome UT examination results. [Adapted from Reference 4.]

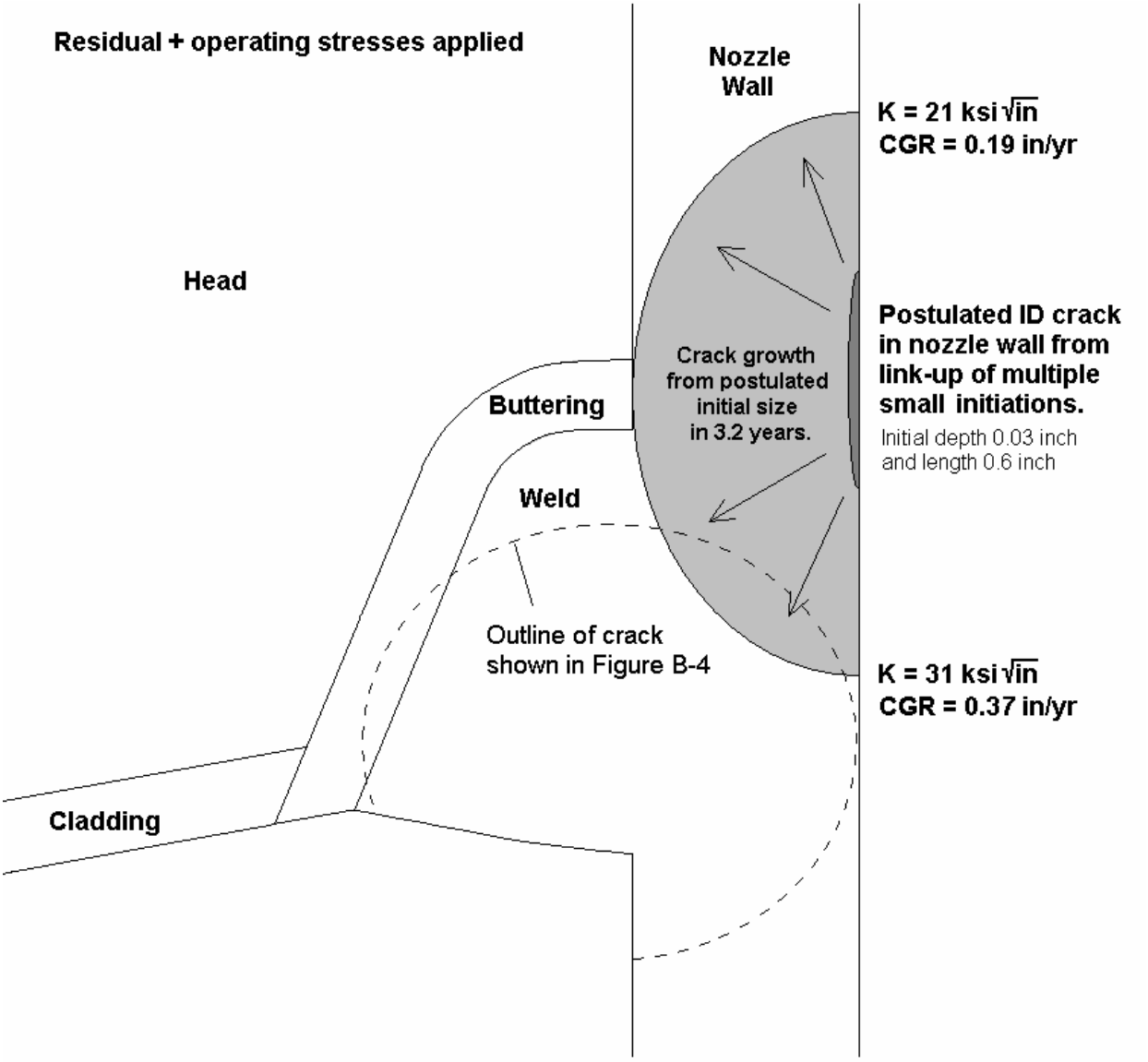

Figure 7. Simulation of growth from a postulated shallow (0.03-inch deep), 0.6-inch long crack at the peak stress location on the nozzle ID to break-through above the top of the weld in 3.2 years. Outline of weld-bottom crack shown in Figure 4 indicates link-up of two such cracks could occur to form a single larger crack.

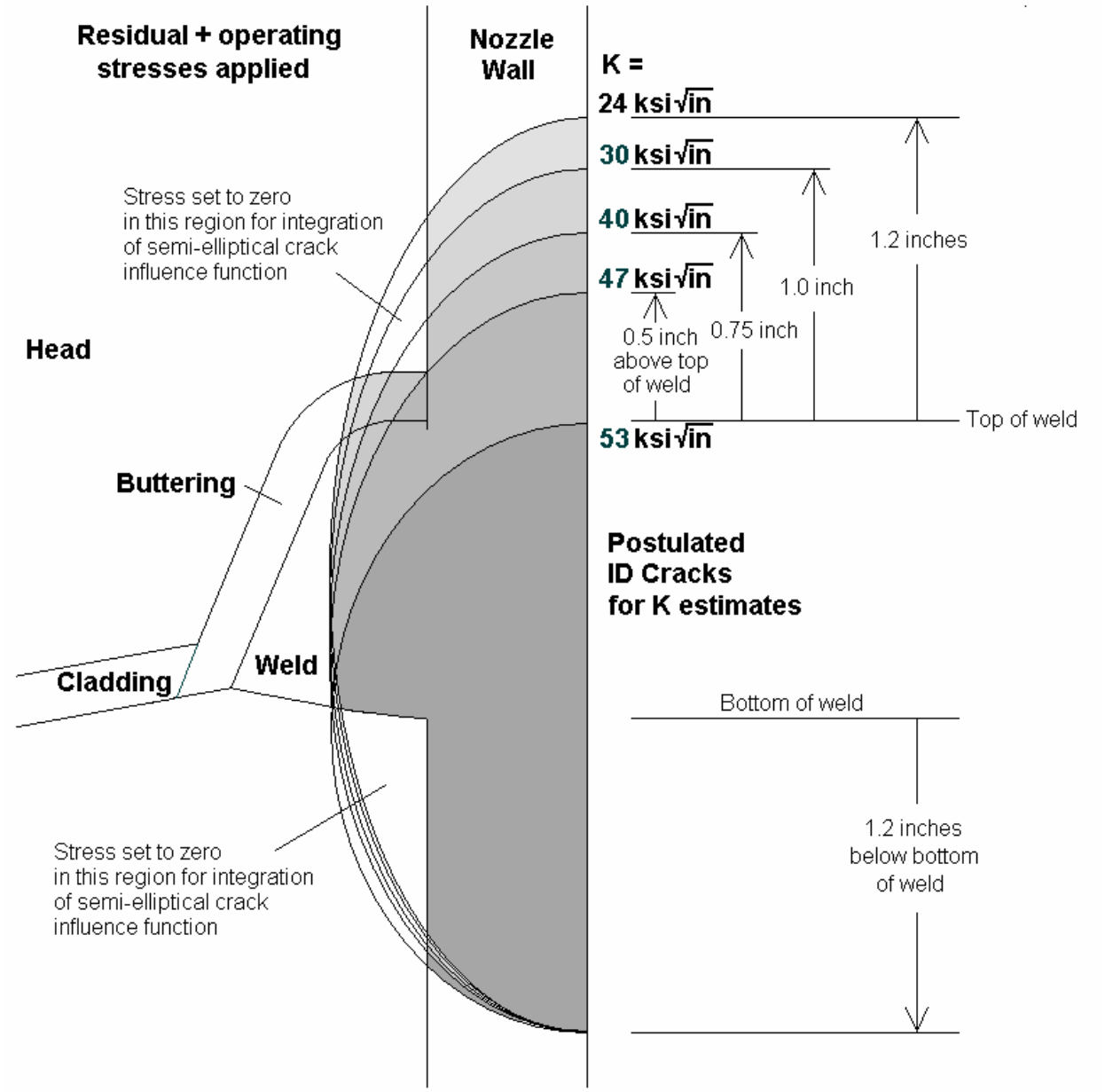

Figure 8. Calculated K-values for a series of deep, semicircular ID cracks in the nozzle, extending into the weld for estimation of crack growth rates and growth time above the top of the weld.

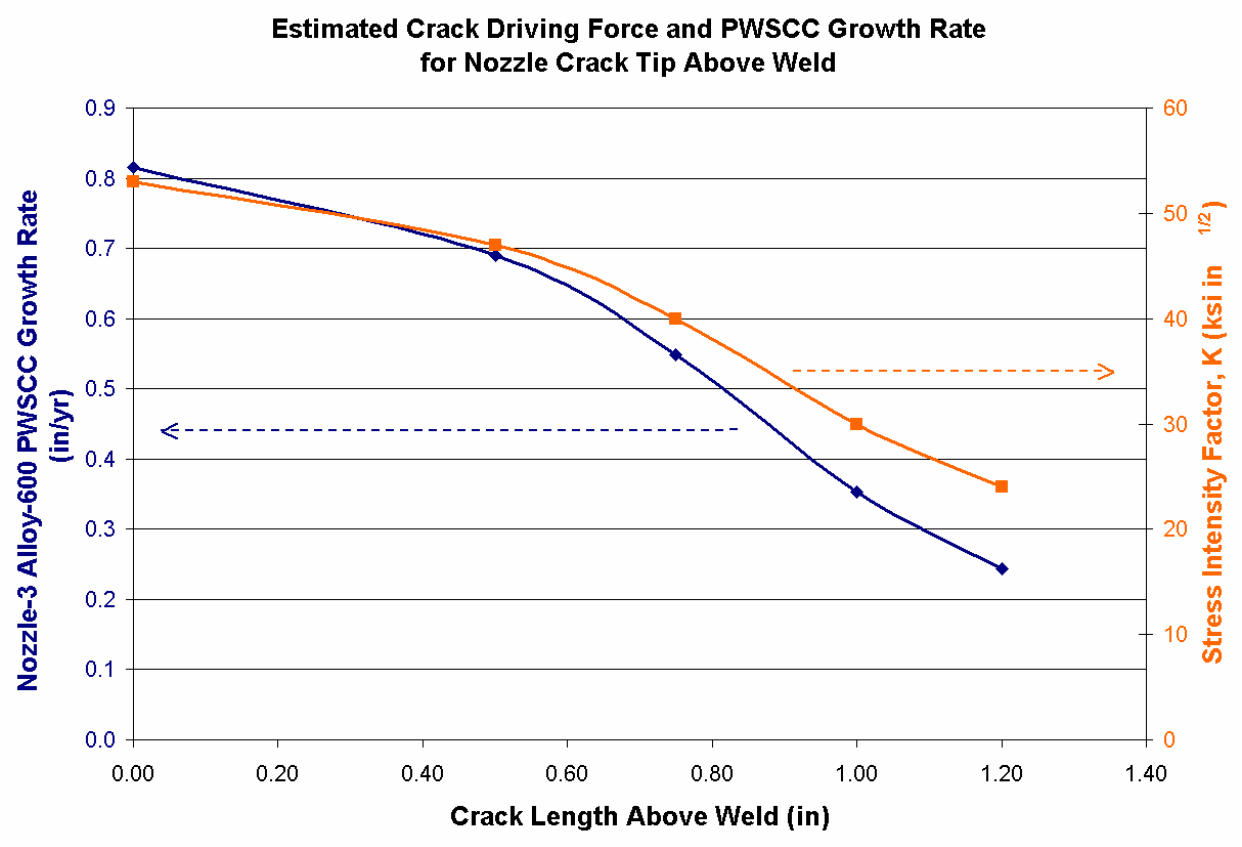

Figure 9. Approximate K-values and corresponding PWSCC growth rates for postulated long ID cracks in the nozzle, extending from 1.2 inches below the weld to the indicated length above the weld, as shown in Figure 8.

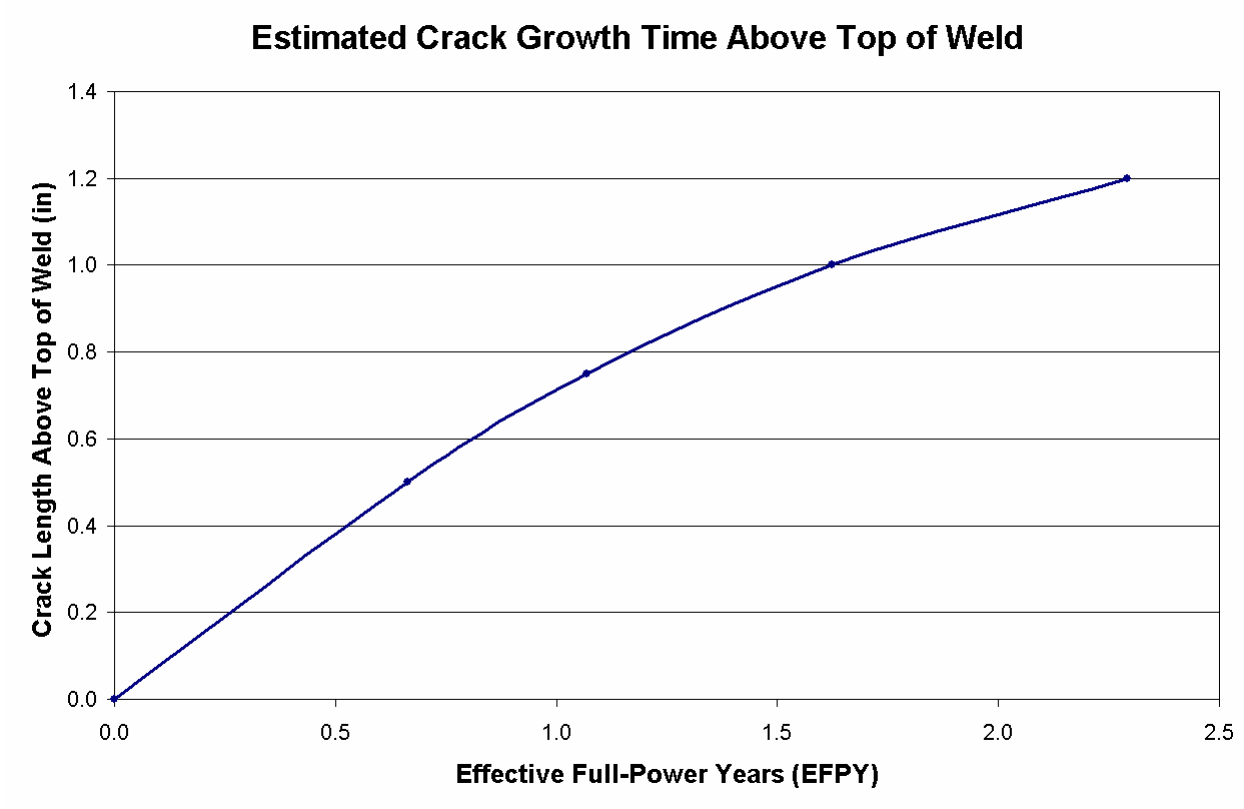

Figure 10. Approximate time in effective full-power years to grow the upper tip of the long axial crack in Nozzle 3 to various lengths above the top of the weld.

References

1. "NASCRAC, NASA Crack Analysis Code," Version 3.2, Exponent, Inc., 1999.

2. B. Alexandreanu et al., "Crack Growth Rates in a PWR Environment of Nickel Alloys from the Davis-Besse and V.C. Summer Power Plants," NUREG/CR-6921, U.S. Nuclear Regulatory Commission, November 2006, at Page 68.

3 "Crack Growth Rates for Evaluating Primary Water Stress Corrosion Cracking (PWSCC) of Alloy 82, 182, and 132 Welds (MRP-115)," EPRI TR-1006696, Electric Power Research Institute, Palo Alto, CA, November 2004, at Page 4-4.

4. M. Hacker, "Davis-Besse CRDM Crack Profiles," Framatome ANP Engineering Information Record No. 51-5018376-00, May 13, 2002.

5 J. Broussard, "Davis Besse CRDM Nozzle Crack Opening Displacement Analysis," Calculation C-5509-00-7, Revision 0, Dominion Engineering, Inc., March 19, 2002, at Page 3 of 7.

6 "Safety Evaluation for B&W-Design Reactor Vessel Head Control Rod Drive Mechanism Nozzle Cracking," BAW-10190P, B&W Nuclear Technologies, May 1993.

7 J. Broussard and D. Gross, "Welding Residual and Operating Stress Analysis of RPV Top and Bottom Head Nozzles," Proceedings of the Conference on Vessel Penetration Inspection, Crack Growth and Repair, NUREG/CP-0191, U.S. Nuclear Regulatory Commission, September 2005.

8 D. Rudland et al., "Analysis of Weld Residual Stresses and Circumferential Through-Wall Crack K-solutions for CRDM Nozzles," Proceedings of the Conference on Vessel Penetration Inspection, Crack Growth and Repair, NUREG/CP-0191, U.S. Nuclear Regulatory Commission, September 2005.